IEEE Access
Multidisciplinary | Rapid Review | Open Access Journal

Received September 14, 2019, accepted October 3, 2019, date of publication October 9, 2019, date of current version October 23, 2019.

Digital Object Identifier 10.1109/ACCESS.2019.2946458

Battery Energy Storage System Based on Incremental Cost Consensus Algorithm for the Frequency Control

CHEN CHEN[1], YU-QING BAO[1], (Member, IEEE), XUE-HUA WU[2], BEIBEI WANG[2], AND CHENG SHEN[1]

[1]NARI School of Electrical Engineering and Automation, Nanjing Normal University, Nanjing 210023, China
[2]School of Electrical Engineering, Southeast University, Nanjing 210096, China

Corresponding author: Yu-Qing Bao (baoyuqing@njnu.edu.cn)

This work was supported in part by the National Natural Science Foundation of China under Grant 51707099, and in part by the Postgraduate Innovation Cultivating Project in Jiangsu Province under Grant SJCX19_0183.

ABSTRACT In the past few years, Battery Energy Storage System (BESS) has been found of great potential in supporting the frequency control. Increasing attentions have been given to the control strategy of BESS. In this paper, a distributed control method considering the life-loss cost is proposed for BESS. Based on the multi-agent system, the Incremental Cost Consensus (ICC) algorithm is applied to minimize the life-loss cost of BESS. In order to improve the control performance, parameters of the system are optimized by Genetic Algorithm (GA). The simulation results are provided to verify the effectiveness of the proposed approach.

INDEX TERMS Frequency control, battery energy storage system, incremental cost consensus algorithm, life-loss cost, genetic algorithm.

I. INTRODUCTION

A large number of Renewable Energy Sources (RESs), such as solar photovoltaic and wind power, have been installed in the power system in recent years. However, the uncontrollable stochastic characteristic of these RESs could be a threat to the frequency stability [1]. Moreover, the voltage magnitude and the rotor angle stability of the power system would be negatively affected by the high penetration of RESs [2]. Under such circumstances, there is an urgent need for controllable resources which can provide timely support. In recent years, Demand Response (DR) has been popular in incorporating with traditional control methods to support the frequency control [3]–[6]. However, most of the DR resources are ON/OFF equipment whose output cannot be adjusted continuously. If a large number of DR resources are turned on or off at the same time, it would cause new disturbances to the power system, thus deteriorating the frequency stability.

A. LITERATURE REVIEW

In the past few years, more researches have focused on the application of Energy Storage Systems (ESSs) to the frequency support of the power system. In [7], ESSs are involved in the primary frequency control and proved to have a quick and stable response to the frequency fluctuation. Among the ESSs, BESS has also got a lot of attention. Combined with the conventional controllers, the BESS in [8] gives better performance than their individual use in stabilizing the system frequency and shortening the settling time. In [9], the BESS is equipped with the inertial and primary frequency control to provide the frequency support in an isolated power system, which is proved effective in arresting the frequency nadir. A Hybrid Energy Storage System (HESS) is introduced in [10] to complement wind generators for the frequency control. The participation of HESS can also achieve higher revenues for providing the frequency support.

It can be seen that many researches have been concentrated on applying distributed consensus control to BESS. Different from the centralized control structure, the distributed control strategy can realize the global information sharing via communication networks between neighboring units. It can reduce the network sensitivity and vulnerability caused by communication failures and enhance the system reliability. The aim of the distributed consensus control is to achieve a general agreement among all units within limited information exchange.

The associate editor coordinating the review of this manuscript and approving it for publication was Chun-Hao Chen.

In [11], the multi-agent-based consensus algorithm is used to control a distributed BESS for the stability of the system frequency. The State-of-Charge (SoC) balance of each battery is achieved, and some units are selected as leaders to transmit the information from the control center. Considering the participation of stochastic renewable power generation, a leader-follower consensus algorithm is introduced in [12] to control the ESSs, which are aggregated to provide the secondary frequency control. The strategy is based on the second-order multi-agent system, with the SoC and the power level selected as the consensus variables. From the simulation results, it can be seen that the consensus-based control scheme performs better than conventional load frequency control methods in the frequency nadir and the recovery time. Reference [13] offers a simple design which is also based on the second-order multi-agent system for ESS. The SoC and the power level are both involved in exchanging information among agents, and together with the consensus control input, they make up a double integrator system. When there is a load change, the consensus design will cooperate with the secondary frequency control to bring the system frequency back to normal.

The papers mentioned above are all devoted to applying consensus-based distributed control methods to BESS for the frequency support. However, the Incremental Cost Consensus (ICC) [14] is not considered in these control strategies, making it a failure to optimize the power and energy allocation according to the dispatch cost of BESS. In this case, the life-loss cost of BESS is not minimal.

The Incremental Cost Consensus (ICC) algorithm is introduced in [14] to solve the Economic Dispatch Problem (EDP). The factors which affect the convergence rate are also analyzed in detail, such as the sampling rate, the convergence coefficient and the communication topologies. The ICC method is adopted in [15] to address the EDP by achieving the agreement among the increment cost of generation units and the increment benefit of flexible loads. References [16]–[18] also take the incremental cost of each unit as the consensus variable to obtain the optimal power allocation. It is worth mentioning that in [18], even if it discards the leader-follower mode and the power mismatch signal to push on, the balance between power supply and demand can still be satisfied and the EDP is solved too. In [19], electric vehicles serve as energy storage devices to provide the energy support for the power grid, and a hierarchical distributed control strategy which involves the ICC algorithm is proposed. The design in this paper is divided into two layers, with the ICC method adopted in the upper layer. In the lower layer, it compares the following three energy allocation methods in terms of the life-loss cost of electric vehicles, which are average allocation method, battery-capacity-based allocation method and ICC-based allocation method. The experimental results show that when the ICC-based allocation approach is adopted in the lower layer, the total life-loss cost of electric vehicles is minimal.

B. CONTRIBUTIONS

A distributed control method based on ICC algorithm is proposed in this paper to minimize the life-loss cost of BESS. The optimal performance of stabilizing the system frequency and reducing the life-loss cost of BESS is obtained by putting GA into effect.

C. ORGANIZATION

The paper is organized as follows. The background knowledge about the control purpose, graph theory and consensus algorithm are presented in Section II as preparations. The ICC algorithm is proposed in Section III. In Section IV, GA is applied to optimize the ICC control strategy. Numerical case studies are provided in Section V. In Section V, a single area power system is introduced in the first subsection. Then the different control methods for BESS, communication topologies and optimization cases are respectively compared in the following three subsections. Conclusions are summarized in Section VI.

II. PROBLEM FORMULATION AND PRELIMINARIES

A. THE PURPOSE OF THE CONSENSUS CONTROL

Lithium Iron Phosphate ($LiFePO_4$) batteries have been a kind of the most popular energy storage devices for their outstanding characteristics, such as high efficiency, superb thermal stability and low cost. They are selected in this research to make up the battery energy storage system. According to the reference [20], the life-loss cost of $LiFePO_4$ battery can be expressed by:

$$C_i = \frac{I_i}{a_i}\left(\frac{Q_i}{Q_{i,\mathrm{N}}}\right)^{b_i} \tag{1}$$

where C_i is the life-loss cost of BESS i; I_i is the initial investment of BESS i; Q_i denotes the output energy of BESS i; $Q_{i,\mathrm{N}}$ represents the rated capacity of BESS i; a_i and b_i are coefficients.

The aim of the economic dispatch strategy is to minimize the total life-loss cost of BESS, which can be calculated as below:

$$\mathrm{Min} \quad C_{\mathrm{total}} = \sum_{i=1}^{n} C_i\left(Q_i\right) \tag{2}$$

where C_{total} is the total life-loss cost of BESS and n is the number of energy storage units.

The output limit constraints which are listed below must be satisfied:

$$\sum_{i=1}^{n} P_i = P_{\mathrm{f}} \tag{3}$$

$$0 \le P_i \le P_{i,\max} \tag{4}$$

where P_i is the output power of unit i; P_{f} is the power information transmitted to BESS and $P_{i,\max}$ is the maximum output power of unit i. The feedback power information can be calculated as following:

$$P_{\mathrm{f}} = -K\Delta f \tag{5}$$

where K and Δf denote the unit regulating power and the frequency deviation of the system respectively.

B. BASICS OF THE CONSENSUS ALGORITHM

The BESS is modelled as a multi-agent system and its network topology can be described by graph theory. A graph G is a pair of disjoint sets [21]:

$$G = (V, E) \tag{6}$$

where V is a set of vertices (nodes) and E is a set of edges between two nodes.

An adjacency matrix is a square matrix used to indicate whether pairs of vertices in the graph are adjacent or not. For a simple graph G on n vertices, the adjacency matrix A is a (0-1)-matrix with zeros on its diagonal. The off-diagonal element a_{ij} is determined by whether there is a connection between node i and node j:

$$a_{ij} = \begin{cases} 1 \text{ (there is a connection between } i \text{ and } j) \\ 0 \text{ (otherwise)} \end{cases} \tag{7}$$

The degree matrix D_e is a diagonal matrix which contains the information about the degree of each node in G. Its diagonal elements d_{ii} are determined by the number of edges attached to each node,

$$d_{ii} = \sum_{i \neq j} a_{ij} \tag{8}$$

Together with the adjacency matrix, the degree matrix is used to create the Laplacian matrix L which contains the information about the dynamic characteristics of G:

$$L = D_e - A \tag{9}$$

A specific state variable is selected as the consensus variable to exchange the information between units. When all consensus variables converge to be equal, it can be said that the consensus is obtained for all nodes and the system has reached a stable state.

Assuming that the information can be exchanged between adjacent units, the information of these vertices can be updated by

$$x_i[k+1] = \sum_{j=1}^{n} q_{ij} x_j[k] \quad i = 1, 2, ..., n \tag{10}$$

where x_i denotes the state variable of node i; k is the discrete time index and q_{ij} is the element determined by Laplacian matrix:

$$q_{ij} = |l_{ij}| / \sum_{j=1}^{n} |l_{ij}| \quad i = 1, 2, ..., n \tag{11}$$

where l_{ij} is the element of the Laplacian matrix.

III. ICC-BASED CONTROL STRATEGY

It is proposed to take the incremental cost per unit time as the consensus variable in this paper. In the unit time, the output energy is equal to the active power numerically. If the cost per unit time is minimized, the cost for a period of time is also the minimum. According to the ICC algorithm proposed in [14], the incremental cost of energy storage batteries can be expressed as:

$$IC_i = \frac{\partial C_i(Q_i)}{\partial Q_i} \quad i = 1, 2, ..., n \tag{12}$$

where IC_i denotes the incremental cost of BESS i.

The novel consensus variable proposed above is shown as below:

$$\lambda_i = IC_i^{'} = \frac{b_i I_i P_i^{b_i - 1}}{a_i P_{i,\mathrm{N}}^{b_i}} \quad i = 1, 2, ..., n \tag{13}$$

where λ_i is the consensus variable; $IC_i^{'}$ is the incremental cost per unit time; P_i denotes the output power of BESS i and $P_{i,\mathrm{N}}$ is the rated capacity after conversion.

The output constraints of the battery can be amended as follows:

$$P_i = \begin{cases} 0 & \left(\frac{\lambda_i a_i P_{i,\mathrm{N}}^{b_i}}{I_i b_i}\right)^{\frac{1}{b_i - 1}} \leq 0 \\ \left(\frac{\lambda_i a_i P_{i,\mathrm{N}}^{b_i}}{I_i b_i}\right)^{\frac{1}{b_i - 1}} & 0 \leq \left(\frac{\lambda_i a_i P_{i,\mathrm{N}}^{b_i}}{I_i b_i}\right)^{\frac{1}{b_i - 1}} \leq P_{i,\max} \\ P_{i,\max} & \left(\frac{\lambda_i a_i P_{i,\mathrm{N}}^{b_i}}{I_i b_i}\right)^{\frac{1}{b_i - 1}} \geq P_{i,\max} \end{cases} \tag{14}$$

The first-order discrete consensus algorithm is updated by the following formulation:

$$\lambda_i[k+1] = \sum_{j=1}^{n} q_{ij} \lambda_j[k] \quad i = 1, 2, ..., n \tag{15}$$

The leader node receives the power signal from control center, and then the information is transmitted to followers through communication networks. The selection of the leader node depends on the number of adjacent nodes each vertex has [22]. The vertex with most adjacent nodes is selected as the leader node and its update rule is modified as:

$$\lambda_i[k+1] = \sum_{j=1}^{n} q_{ij} \lambda_j[k] + \varepsilon \Delta P \tag{16}$$

$$\Delta P = P_f - \sum_{i=1}^{n} P_i \tag{17}$$

where ε is a positive scalar called convergence coefficient which determines the convergence speed of the leader; ΔP denotes the mismatch power between the demand and generation.

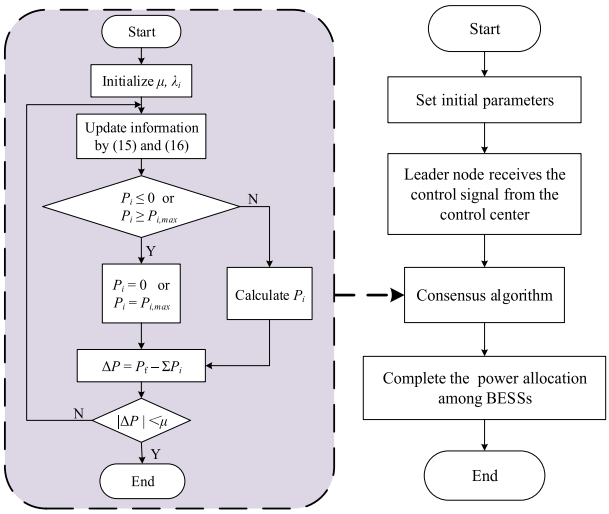

FIGURE 1. The flowchart of the consensus algorithm.

The flowchart of the ICC-based distributed control strategy is presented in Fig. 1. The scheduling information is sent from the control center to the leader node, and then the power allocation is completed by putting ICC algorithm into effect. The ICC algorithm will run until the power balance between the BESS supply and the system demand is satisfied.

The proposed ICC algorithm is summarized in Algorithm 1.

Algorithm 1 The ICC algorithm on the ith unit

1: Initialize the parameters ($\lambda_i(k)$, $P_i(k)$, $P_{i,\mathrm{N}}$ and ε)
2: **for** $k = 1, 2, \ldots, M$ **do**
3: Measure the frequency deviation $\Delta f(k)$ in the system
4: Compute the mismatch power by (5) and (17)
5: Receive the consensus state $\lambda_j(k\text{-}1)$ from its neighbors, $j \in \mathrm{N}_i$
6: Send the local consensus state $\lambda_i(k\text{-}1)$ to its neighbors
7: **if** it is the leader node
8: Update the consensus state by (16)
9: **else**
10: Update the consensus state by (15)
11: **end if**
12: Calculate the output power of BESS by (14)
13: **end for**

IV. GA-BASED OPTIMIZATION

In this section, parameters are optimized to improve the system performance. The droop parameter R is fixed by the requirement of the primary frequency control. Only K_{I} (the integral gain of the automatic generation control) and ε (the convergence coefficient) can be reset to improve the performance, and the value of ε would directly affect the performance of BESS.

Genetic Algorithm (GA) is a stochastic optimization algorithm based on the principles of evolution. In GA, an individual (chromosome) represents a valid solution to the problem. The fitness value is used to measure an individual's adaptation level to the living environment. It is calculated by the fitness function and associated with the objective function. The greater the fitness value is, the better the individual adapts to the environment. The optimal solution is completed by three operators which are selection, crossover and mutation. The selection operator is to the retain the outstanding individuals and eliminate the inferior ones in the population. It is based on each individual's fitness value. Popular methods include the roulette wheel selection and the elitist model. The crossover operator exchanges the genes in the same position between two selected individuals to generate a new individual. It plays a key role and greatly improves the searching ability of GA. The mutation operator is to change the genes of individuals, and then the mutated new population will participate in the next evolution. It ensures the diversity of the offspring.

There is no need to consider the specific internal working modes when searching the global optimal result. GA has been widely used in optimization designs due to its high efficiency and great flexibility [23]. The problem here is a nonlinear optimization process, which needs to consider the dynamic characteristics of multi-agents. Therefore, GA is preferred to traditional optimization methods in this paper.

The steps to implement GA method can be summarized as following:

Step 1: Randomize an initial set of chromosomes.

Step 2: Calculate the fitness of each individual and find the fittest members.

Step 3: Execute crossover and mutation operations.

Step 4: Return to Step 2 until the terminal condition is satisfied.

The realization of GA-based optimization is presented in Algorithm 2.

Algorithm 2 GA-based Optimization

1: Generate an initial population randomly
2: **while** the terminal criterion is False **do**
3: Calculate the fitness of the population
4: Select the fittest members according to the fitness value
5: Reproduce the next population
6: Perform crossover and mutation operators on the reproduced population
7: **end while**

Considering the actual situation, it is essential to calculate as many scenarios as possible in the optimization process. Reference [6] takes six simple and basic scenarios into account in its three-area power system. In this case, scenarios are designed for the objective function. These scenarios are suitable for the case here and can be modified for actual situations.

An objective function should be determined to activate the process of optimization. The Integral Square Error (ISE) of the frequency deviation and the total life-loss cost are both considered in the objective function:

$$\text{Min} \sum_{s=1}^{N_S} \left(w_{s1} \sum_{i=1}^{n} C_i + w_{s2} \int_0^T \Delta f^2 dt \right) \tag{18}$$

where N_s denotes the number of scenarios; w_{s1} and w_{s2} are weight factors.

The parameters of GA are listed in Table 1.

TABLE 1. Parameters of genetic algorithm.

Parameter	Value
Population size	80
Elite count	7
Crossover rate	0.9
Mutation rate	0.3
Generations	30
StallGenLimit	30
TolFun	5e-100

V. CASE STUDIES

In this section, case studies are conducted in MATLAB to verify the effectiveness of the proposed strategy. Based on the matrix mode, MATLAB can process large amounts of data efficiently. It integrates computation and visualization, and can be combined with other programming software, breaking through the shortcomings of traditional interactive programming languages.

A. MODEL DEVELOPMENT

A single area power system equipped with BESS is depicted in Fig. 2. It can be seen that BESS is involved in the primary frequency support.

K_I is the integral gain of the secondary frequency control; s is the laplace operator; P_{sp} is the power setpoint calculated by the secondary frequency control; R is the speed droop parameter; T_g is the speed governor time constant; ΔY is the gate position deviation; T_r is the reheat time constant; F_{HP} is the power fraction of the HP turbine section; ΔP_r is the thermal power deviation of reheated turbines; T_t is the turbine time constant; ΔP_m is the mechanical power deviation of generators; H is the generator inertia; D is the load-damping factor; Δf is the frequency deviation; P_{BESS} is the output power of the BESS; ΔP_d is the disturbance power ($\Delta P_d > 0$ for a sudden increase in load and $\Delta P_d < 0$ for a sudden increase in generation).

The model of the power system can be described by the following state-space equations, which are realized by Euler method.

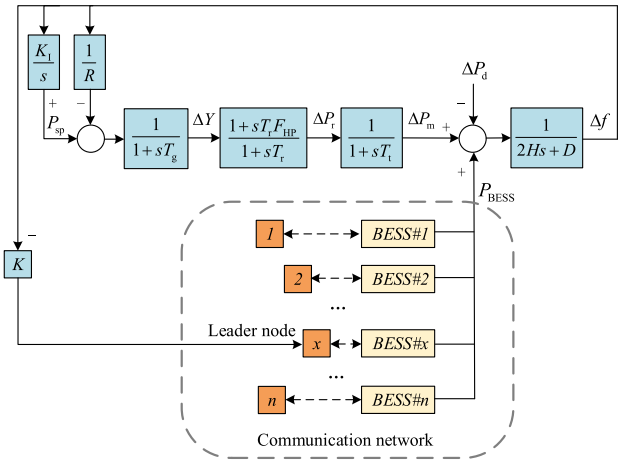

FIGURE 2. A single area frequency response model with BESS.

$$\begin{cases} \dot{X} = AX + BU + R\Delta P_d \\ Y = CX \end{cases} \tag{19}$$

where

$$X = [P_{sp} \quad \Delta Y \quad \Delta P_r \quad \Delta P_m \quad \Delta f]^T$$

$$A = \begin{bmatrix} 0 & 0 & 0 & 0 & -K_I \\ \frac{1}{T_g} & -\frac{1}{T_g} & 0 & 0 & -\frac{1}{T_g R} \\ \frac{F_{HP}}{T_g} & \frac{1}{T_r} - \frac{F_{HP}}{T_g} & -\frac{1}{T_r} & 0 & -\frac{F_{HP}}{T_g R} \\ 0 & 0 & \frac{1}{T_t} & -\frac{1}{T_t} & 0 \\ 0 & 0 & 0 & \frac{1}{2H} & -\frac{D}{2H} \end{bmatrix}$$

$$B = \begin{bmatrix} 0 & 0 & 0 & 0 & \frac{1}{2H} \end{bmatrix}^T \qquad R = \begin{bmatrix} 0 & 0 & 0 & 0 & -\frac{1}{2H} \end{bmatrix}^T$$

$$C = \begin{bmatrix} 0 & 0 & 0 & 0 & 1 \end{bmatrix} \qquad U = P_{BESS}$$

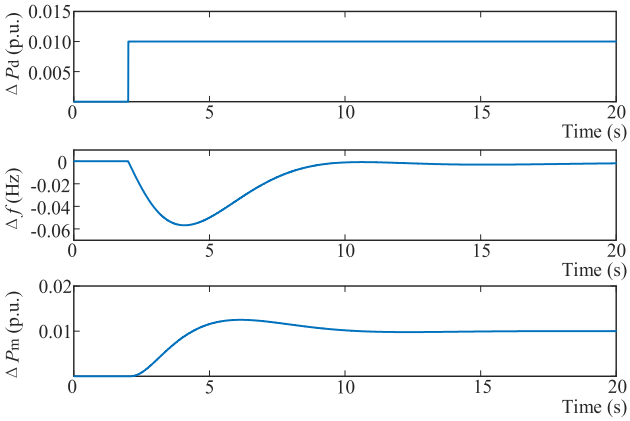

FIGURE 3. Frequency response to a sudden disturbance.

Considering the nominal frequency of 50 Hz, Fig. 3 shows the regulation process of the power system. The frequency

drops when a load increase ($\Delta P_d > 0$) suddenly occurs, and then the speed governors increase the output power of generators according to the frequency deviation. Although the primary frequency regulation responds quickly to the frequency fluctuation, it cannot eliminate it completely. In combination with the primary control, the secondary frequency regulation can restore the frequency to the nominal value. However, it often takes more than one minute for secondary regulation to respond, thus BESS can provide immediate support at the time of load disturbances.

When there is a sudden disturbance, the generators and BESS would respond according to the frequency fluctuation. Based on (5), the frequency deviation signal is converted into power information which is transmitted to the leader node of BESS. Power allocation is completed by ICC algorithm to minimize the total life-loss cost of BESS. Then the output power information of follower nodes will be dispatched through communication networks. The parameters of the power system and BESS [24] are respectively listed in the appendix and Table 2.

TABLE 2. Parameters of the battery energy storage system.

Unit	a_i	b_i	$Q_{i,N}$ (KW • h)
1	1.53×10^3	2.39	4.32
2	1.70×10^3	2.10	8.15
3	1.82×10^3	2.45	1.47
4	1.36×10^3	2.12	6.97
5	1.75×10^3	1.83	9.89

B. COMPARISON OF THE CONTROL METHODS FOR BESS

The performance of the ICC algorithm is examined in this part. The topology of the BESS is shown in Fig. 4, with the communication connections represented by dotted lines. The following 4 cases are considered for comparison.

Case 1: No BESS participates in the frequency control.

Case 2: The average allocation method is adopted for BESS to participate in the frequency control.

Case 3: The second-order consensus control method proposed in [13] is adopted for BESS to participate in the frequency control.

Case 4: The distributed control strategy based on ICC algorithm is adopted for BESS to participate in the frequency control.

The communication time-step-size between units is set to 0.005s. Considering 3% step disturbance ($\Delta P_d = 0.03$p.u.) at 0.1s, the simulation results are shown in Fig. 5 and Table 3. The following conclusions can be drawn from the simulation results:

- Compared with the case without BESS (Case 1), cases with BESS (Case 2, 3 and 4) tend to have a smaller frequency deviation. For cases with BESS, although the frequency nadir of Case 4 is a little worse than the other two cases, there is no significant difference in the frequency response between the three control methods.
- Under the circumstance of little difference in the overall output of BESS, the total life-loss cost of BESS in Case 4 is the lowest. The average allocation method (Case 2) and the second-order consensus control approach (Case 3) both cost more than 5 yuan, while the distributed control strategy based on ICC algorithm (Case 4) only costs 4.4805 yuan.

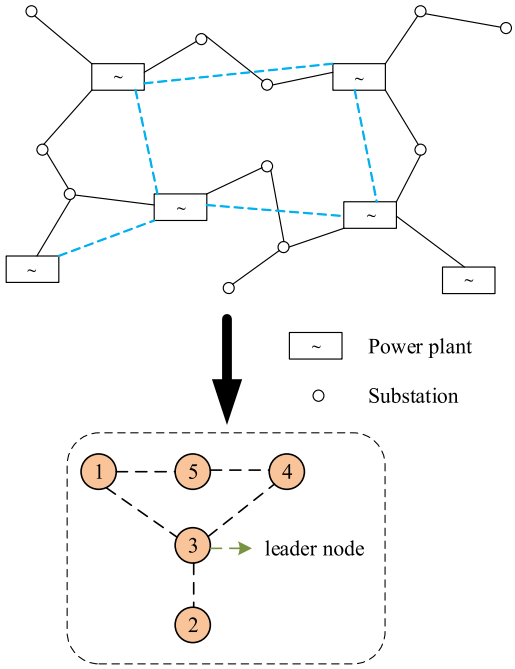

FIGURE 4. The communication topology of the BESS.

TABLE 3. The maximum frequency deviation and life-loss cost in each case.

Case No.	Maximum frequency deviation (Hz)	Total life-loss cost (yuan)
Case1	0.1702	
Case2	0.1441	5.1746
Case3	0.1443	5.2379
Case4	0.1444	4.4805

Taking both the frequency control and the life-loss cost into consideration, the proposed method in Case 4 does have an obvious advantage. In the case of the similar frequency response, the distributed control strategy based on ICC algorithm performs better in saving the life-loss cost of BESS than the other two methods.

C. COMPARISON OF THE DIFFERENT COMMUNICAITON TOPOLOGIES

This subsection aims to evaluate the influence of different topologies on the performance of BESS. The algebraic

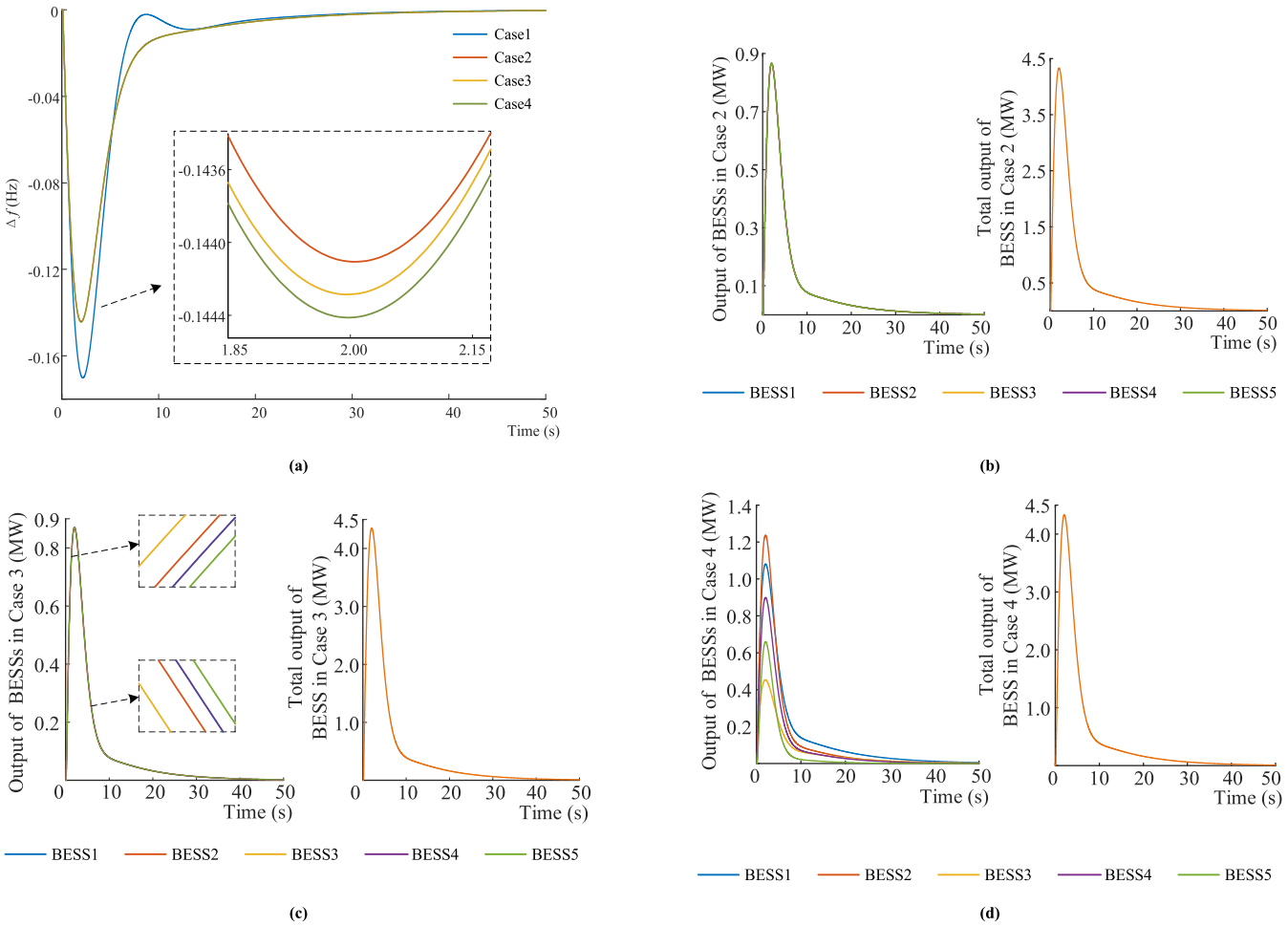

FIGURE 5. Simulation results of different control methods: (a) the frequency deviation of 4 cases; (b) output of BESSs in Case 2; (c) output of BESSs in Case 3; (d) output of BESSs in Case 4.

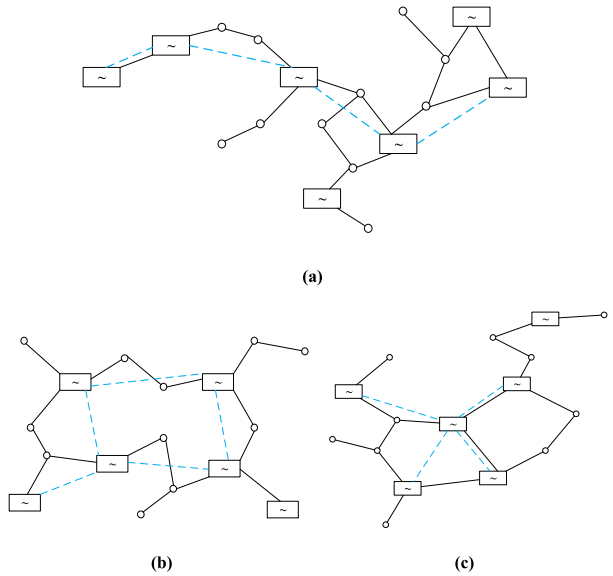

FIGURE 6. Topologies of the 3 cases: (a) the topology of Case 1; (b) the topology of Case 2; (c) the topology of Case 3.

connectivity of the graph is equal to the minimum non-zero eigenvalue of the Laplacian matrix, which is a description of the network structure of the graph. The consensus algorithm characterizes the convergence speed of the system through the algebraic connectivity [25]. Three cases are designed to make the contrast, with the communication graphs depicted in Fig. 6. In order to ensure the accuracy and rationality of the results, the BESS parameters in the following 3 cases are set to be the same.

Case 1: The algebraic connectivity of the topology 1 in Fig. 6 (a) is 0.3820.

Case 2: The algebraic connectivity of the topology 2 in Fig. 6 (b) is 0.8299.

Case 3: The algebraic connectivity of the topology 3 in Fig. 6 (c) is 1.

The communication time-step-size between units is expanded to 0.08s. Considering 3% step disturbance ($\Delta P_{\mathrm{d}} = 0.03$p.u.) at 0.1s, the simulation results are presented in Fig. 7 and the related data are listed in Table 4. The following observations can be obtained:

- The speed at which the system achieves agreement is greatly affected by the algebraic connectivity. Compared with Case 1 and Case 2, there is an earlier trend for the consensus variables to converge in Case 3. According to the three diagrams of the consensus state, the larger the algebraic connectivity is, the faster the system converges.

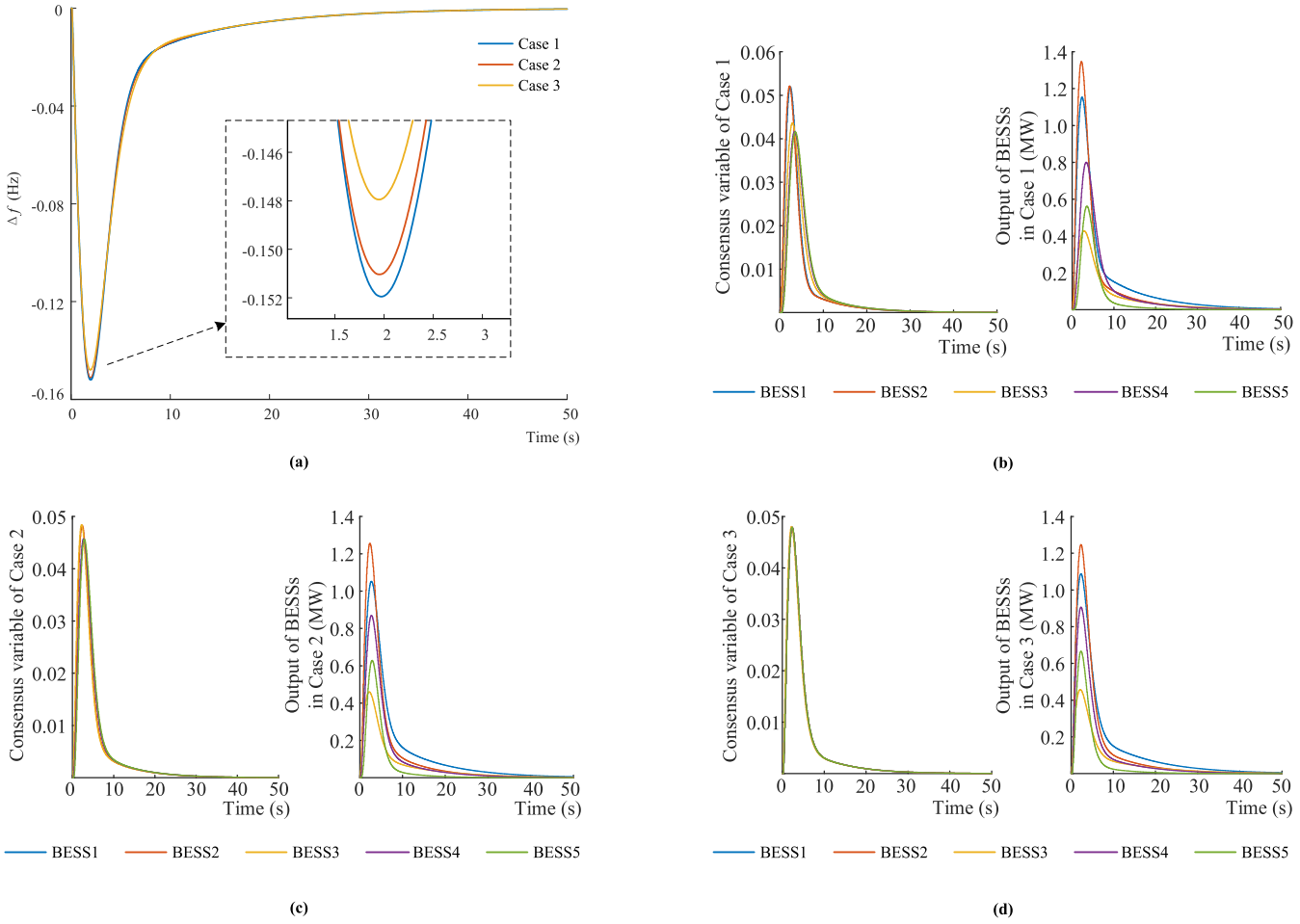

FIGURE 7. Simulation results of using different topologies: (a) the frequency deviation of 3 cases; (b) output of BESS in Case 1; (c) output of BESS in Case 2; (d) output of BESS in Case 3.

TABLE 4. The maximum frequency deviation and life-loss cost in each case.

Case No.	Algebraic connectivity	Maximum frequency deviation (Hz)	Total life-loss cost (yuan)
Case1	0.3820	0.1520	4.5233
Case2	0.8299	0.1510	4.5041
Case3	1.0000	0.1479	4.4864

- In the 3 cases, the system with larger algebraic connectivity tends to result in a smaller frequency deviation. As the algebraic connectivity increases, the maximum frequency deviation of the system decreases.
- In terms of the life-loss cost of BESS, the system with larger algebraic connectivity tends to cost less. With the increase of the algebraic connectivity, the life-loss cost of BESS decreases too.

From the analysis above, it can be concluded that the communication network with larger algebraic connectivity is superior in terms of the frequency stability, speeding up the convergence and saving the life-loss cost of BESS.

D. COMPARISON OF THE OPTIMIZATON CASES

In this subsection, GA is utilized to achieve the optimal performance of the system. The objection function adopts (18), with the communication time-step-size between units set to 0.2s. Based on the communication topology used in Fig. 4, the following 3 cases are compared to examine the effectiveness of the optimization.

Case 1: The parameters K_I and ε refer to [26] and [15] respectively (determined without optimization).

Case 2: Only the parameter K_I is optimized by GA.

Case 3: The parameters K_I and ε are both optimized by GA.

Considering 3% step disturbance ($\Delta P_d = 0.03$p.u.) at 0.1s, the simulation results are provided in Fig. 8 and the relevant data are listed in Table 5. It can be seen that:

- It can be seen that the optimized systems (Case 2 and Case 3) tend to have a smaller frequency deviation than the un-optimized one (Case 1). Additionally, involving both K_I and ε in the optimization (Case 3) can further reduce the maximum frequency deviation.

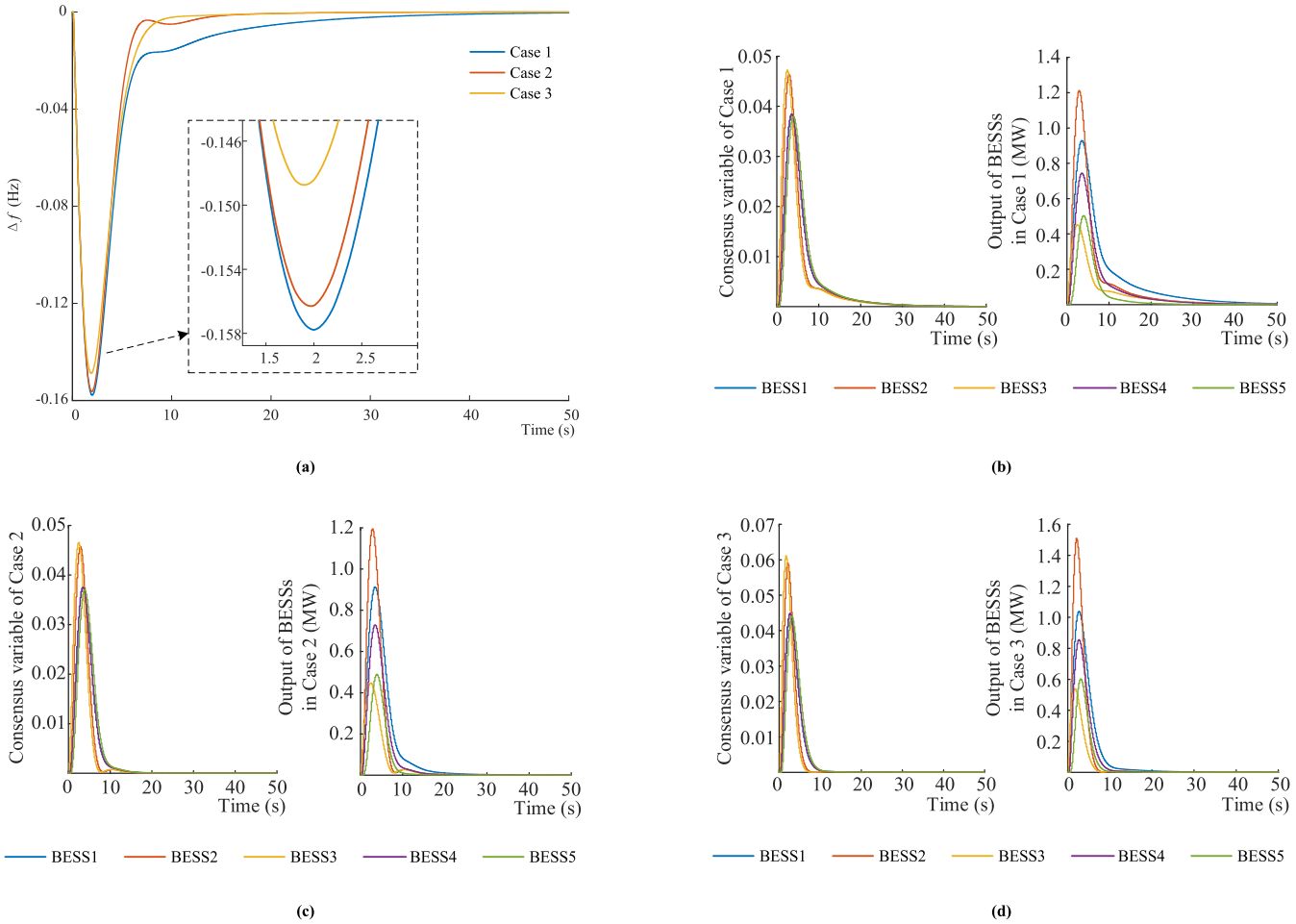

FIGURE 8. Simulation results of different optimization methods: (a) the frequency deviation of 3 cases; (b) output of BESS in Case 1; (c) output of BESS in Case 2; (d) output of BESS in Case 3.

TABLE 5. The maximum frequency deviation and life-loss cost in each case.

Case No.	K_1	ε	Maximum frequency deviation (Hz)	Total life-loss cost (yuan)
Case1	1.91	0.005	0.1578	4.5680
Case2	2.65	0.005	0.1563	2.0804
Case3	2.65	0.013	0.1487	2.0279

- From the respect of the frequency response, the optimized systems (Case 2 and Case 3) tend to have a shorter settling time than the un-optimized one (Case 1). The un-optimized system frequency fails to recover to the rated value within 40 seconds, while the optimized ones can be stabilized within 20 seconds. For optimized cases, Case 3 takes less time than Case 2. From the respect of the convergence rate of BESS, the optimized systems converge faster than the un-optimized one, which can be judged from the state of the consensus variable. The un-optimized case takes more than 30 seconds to reach the agreement, while the optimized ones less than 20 seconds. In addition, curves of the consensus variables and the output power of Case 3 are smoother than those in Case 1 and Case 2.
- In terms of saving the life-loss cost of BESS, the effect of the GA-based optimization method is remarkable. The life-loss cost of the un-optimized case (Case 1) is more than twice as much as the optimized ones (Case 2 and Case 3), with Case 3 the lowest.

GA-based optimization method has proved to be effective in stabilizing the system frequency, speeding up the system convergence and saving the life-loss cost of BESS. Besides, the parameter ε directly affects the performance of the BESS, so engaging it in the optimization improves the comprehensive performance of the system.

VI. CONCLUSION

In this paper, an economical distributed control strategy is designed for BESS to participate in the frequency control. Compared with the existing studies, the main contribution of this paper can be summarized as following:

- A novel distributed control strategy of BESS based on ICC for the frequency control is proposed. Compared with the existing methods (e.g. [13]), the ICC-based control strategy can help reduce the scheduling cost of BESS.
- GA is utilized to obtain the optimal solution of the system. It is proved to be effective on the frequency stability, speeding up the convergence and saving the life-loss cost.

The future work may focus on other optimization methods to improve the proposed method.

APPENDIX

The parameters of the single area power system on 800MW base are as follows:

K_{I}= 1.91, $R = 0.05$, $T_{\mathrm{g}} = 0.2$, $T_{\mathrm{r}} = 7$,
$F_{\mathrm{HP}} = 0.3$, $T_{\mathrm{t}} = 0.3$, $H = 5$, $D = 1$, $K = 30$

REFERENCES

[1] L. Zhang, G. Chen, Z. Wang, Z. Dong, and D. Hill, "Robust H_∞ load frequency control of future power grid with energy storage considering parametric uncertainty and time delay," in *Proc. IEEE PES Gen. Meeting | Conf. Expo.*, National Harbor, MD, USA, Jul. 2014, pp. 1–5.

[2] R. Shah, N. Mithulananthan, R. C. Bansal, and V. K. Ramachandaramurthy, "A review of key power system stability challenges for large-scale PV integration," *Renew. Sustain. Energy Rev.*, vol. 41, pp. 1423–1436, Jan. 2015.

[3] Y.-Q. Bao, Y. Li, Y.-Y. Hong, and B. Wang, "Design of a hybrid hierarchical demand response control scheme for the frequency control," *IET Gener., Transmiss. Distrib.*, vol. 9, no. 15, pp. 2303–2310, Nov. 2015.

[4] M. S. U. Zaman, S. B. A. Bukhari, K. M. Hazazi, Z. M. Haider, R. Haider, and C.-H. Kim, "Frequency response analysis of a single-area power system with a modified LFC model considering demand response and virtual inertia ," *Energies*, vol. 11, no. 4, p. 787, Mar. 2018.

[5] V. Lakshmanan, M. Marinelli, J. Hu, and H. W. Bindner, "Provision of secondary frequency control via demand response activation on thermostatically controlled loads: Solutions and experiences from Denmark," *Appl. Energy*, vol. 173, pp. 470–480, Jul. 2016.

[6] Y.-Q. Bao, Y. Li, B. Wang, M. Hu, and P. Chen, "Demand response for frequency control of multi-area power system," *J. Mod. Power Syst. Clean Energy*, vol. 5, no. 1, pp. 20–29, Jan. 2017.

[7] H.-J. Moon, A.-Y. Yun, E.-S. Kim, and S.-I. Moon, "An analysis of energy storage systems for primary frequency control of power systems in South Korea," in *Proc. 3rd Int. Conf. Energy Environ. Res.*, Barcelona, Spain, 2017, pp. 116–121.

[8] P. Prajapati and A. Parmar, "Multi-area load frequency control by various conventional controller using battery energy storage system," in *Proc. Int. Conf. Energy Efficient Technol. Sustainability*, Nagercoil, India, Apr. 2016, pp. 467–472.

[9] M. Ramírez, R. Castellanos, J. G. Calderón, and O. P. Malik, "Battery energy storage for frequency support in the BCS electric power system," in *Proc. IEEE PES Transmiss. Distrib. Conf. Exhib.-Latin Amer.*, Lima, Peru, Sep. 2018, pp. 1–5.

[10] S. M. Vaca, C. Patsios, and P. Taylor, "Enhancing frequency response of wind farms using hybrid energy storage systems," in *Proc. IEEE Int. Conf. Renew. Energy Res. Appl.*, Birmingham, U.K., Nov. 2016, pp. 325–329.

[11] H. Yang, S. Li, Q. Li, and W. Chen, "Hierarchical distributed control for decentralized battery energy storage system based on consensus algorithm with pinning node," *Protection Control Mod. Power Syst.*, vol. 3, p. 6, Dec. 2018.

[12] Y. Wang, Y. Xu, Y. Tang, K. Liao, M. H. Syed, E. Guillo-Sansano, and G. M. Burt, "Aggregated energy storage for power system frequency control: A finite-time consensus approach," *IEEE Trans. Smart Grid*, vol. 10, no. 4, pp. 3675–3686, Jul. 2019.

[13] J. Khazaei and Z. Miao, "Consensus control for energy storage systems," *IEEE Trans. Smart Grid*, vol. 9, no. 4, pp. 3009–3017, Jul. 2018.

[14] Z. Zhang and M.-Y. Chow, "Convergence analysis of the incremental cost consensus algorithm under different communication network topologies in a smart grid," *IEEE Trans. Power Syst.*, vol. 27, no. 4, pp. 1761–1768, Nov. 2012.

[15] J. Xie, K. Chen, D. Yue, Y. Li, K. Wang, S. Weng, and C. Huang, "Distributed economic dispatch based on consensus algorithm of multi agent system for power system," *Electr. Power Autom. Equip.*, vol. 36, no. 2, pp. 112–117, Feb. 2016.

[16] R. Wang, Q. Li, B. Zhang, and L. Wang, "Distributed consensus based algorithm for economic dispatch in a microgrid," *IEEE Trans. Smart Grid*, vol. 10, no. 4, pp. 3630–3640, Jul. 2019.

[17] W. Chen and T. Li, "A distributed economic dispatch algorithm based on multi-agent consensus control and incremental power supplying," *IFAC-PapersOnLine*, vol. 51, no. 23, pp. 7–12, Dec. 2018.

[18] Z. Yang, J. Xiang, and Y. Li, "Distributed consensus based supply-demand balance algorithm for economic dispatch problem in a smart grid with switching graph," *IEEE Trans. Ind. Electron.*, vol. 64, no. 2, pp. 1600–1610, Feb. 2017.

[19] M. Wu, Y. Q. Bao, G. Chen, J. Zhang, B. Wang, and W. Qian, "Hierarchical distributed control strategy for electric vehicle mobile energy storage clusters," *Energies*, vol. 12, no. 7, p. 1195, Mar. 2019.

[20] G. Chen, Y. Bao, J. Zhang, B. Wang, M. Wu, and T. Wang, "Distributed cooperative control strategy for energy storage units considering life loss cost," *Power Syst. Technol.*, vol. 42, no. 5, pp. 1495–1501, May 2018.

[21] P. Kolaric, C. Chen, A. Dalal, and F. L. Lewis, "Consensus controller for multi-UAV navigation," *Control Theory Technol.*, vol. 16, no. 2, pp. 110–121, May 2018.

[22] S. Kar and G. Hug, "Distributed robust economic dispatch in power systems: A consensus + innovations approach," in *Proc. IEEE Power Energy Soc. Gen. Meeting*, San Diego, CA, USA, Jul. 2012, pp. 1–8.

[23] P. Guo, X. Wang, and Y. Han, "The enhanced genetic algorithms for the optimization design," in *Proc. 3rd Int. Conf. Biomed. Eng. Inform.*, Yantai, China, 2010, pp. 2990–2994.

[24] I. Duggal and B. Venkatesh, "Short-term scheduling of thermal generators and battery storage with depth of discharge-based cost model," *IEEE Trans. Power Syst.*, vol. 30, no. 4, pp. 2110–2118, Jul. 2015.

[25] R. Olfati-Saber, J. A. Fax, and R. M. Murray, "Consensus and cooperation in networked multi-agent systems," *Proc. IEEE*, vol. 95, no. 1, pp. 215–233, Jan. 2007.

[26] Y.-Q. Bao, C. Shen, Q. Wang, and J.-L. Zhang, "Demand response based on Kalman-filtering for the frequency control," *J. Elect. Eng. Technol.*, vol. 14, no. 3, pp. 1087–1094, May 2019.

CHEN CHEN was born in Yancheng, China, in 1996. She received the B.S. degree from Nanjing Normal University (NJNU), Nanjing, China, in June 2018, where she is currently pursuing the M.S. degree. Her current research interests include the frequency control of the power systems and the consensus control for multiagent systems.

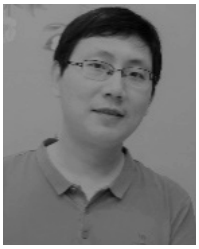

YU-QING BAO was born in Zhenjiang, China, in 1987. He received the Ph.D. degree from Southeast University (SEU), Nanjing, China, in March 2016. He is currently an Associate Professor with Nanjing Normal University (NJNU). His current research interests include power system operation and scheduling, power demand side management, and the frequency control of the power systems.

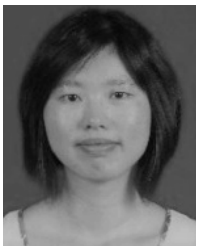

XUE-HUA WU received the B.S. degree in electrical engineering and the M.S. degree in power system and its automation from the Nanjing University of Aeronautics and Astronautics (NUAA), Nanjing, China, in 2009 and 2012, respectively. She is currently pursuing the Ph.D. degree in electrical engineering with Southeast University (SEU), Nanjing, China. Her research interest includes machine learning and its application in electrical engineering.

BEIBEI WANG received the Ph.D. degree in electric power engineering from Southeast University (SEU), Nanjing, China, in 2007, where she has been an Associate Professor, since June 2007. Prior to joining SEU, she was with NARI, from 2003 to 2004. She worked as a Visiting Scholar with the Department of Geography and Environmental Engineering, Johns Hopkins University, from September 2012 to September 2013. Her current interests include power market and demand side management.

CHENG SHEN was born in Bozhou, China, in 1996. He received the B.S. degree from Tianjin Polytechnic University (TJPU), Tianjin, China, in June 2016. He is currently pursuing the M.S. degree with Nanjing Normal University (NJNU). His current research interest includes the operation and control of the power systems.